CODEN IEJMAT *Internet Electronic Journal of Molecular Design* **2008**, *7*, 142–151 ISSN 1538–6414
BioChem Press http://www.biochempress.com

Inter*net* Electronic Journal of Molecular Design

July 2008, Volume 7, Number 7, Pages 142–151

Editor: Ovidiu Ivanciuc

Three–Dimensional Molecular Field Analysis of Dihydroindazolocarbazole Analogues of KDR and Tie–2 Receptor Tyrosine Kinase Inhibitors

Neha Kansal,[1] Om Silakari,[1] and Muttineni Ravikumar [2]

[1] Department of Pharmaceutical Science and Drug Research, Punjabi University, Patiala 147–002, Punjab, India
[2] GVK Biosciences Pvt. Ltd., #210 'My Home Tycoon', 6–3–1192 Begumpet, Hyderabad 500 016, India

Received: July 2, 2007; Accepted: July 24, 2007; Published: July 31, 2008

Citation of the article:
N. Kansal, O. Silakari, and M Ravikumar, Three–Dimensional Molecular Field Analysis of Dihydroindazolocarbazole Analogues of KDR and Tie–2 Receptor Tyrosine Kinase Inhibitors, *Internet Electron. J. Mol. Des.* **2008**, *7*, 142–151, http://www.biochempress.com.

Inter*net* Electronic Journal of Molecular Design

BioChem Press
http://www.biochempress.com

Three–Dimensional Molecular Field Analysis of Dihydroindazolocarbazole Analogues of KDR and Tie–2 Receptor Tyrosine Kinase Inhibitors

Neha Kansal,[1] Om Silakari,[1,*] and Muttineni Ravikumar[2]

[1] Department of Pharmaceutical Science and Drug Research, Punjabi University, Patiala 147–002, Punjab, India

[2] GVK Biosciences Pvt. Ltd., #210 'My Home Tycoon', 6–3–1192 Begumpet, Hyderabad 500 016, India

Received: July 2, 2007; Accepted: July 24, 2007; Published: July 31, 2008

Internet Electron. J. Mol. Des. **2008**, *7* (7), 142–151

Abstract

Motivation. Angiogenesis, the formation of new blood vessels from pre–existing vessels has been considered a critical event for growth and metastasis of solid tumors. KDR and Tie–2 are two receptor tyrosine kinases (RTK) that play primary role in tumor angiogenesis. Due to the vital role of RTK signaling in tumor progression, inhibition of RTK signaling pathways emerged as one of the most compelling targets for therapeutic intervention in cancer. A set of dihydroindazolocarbazole analogues reported as RTK inhibitors were analyzed by employing molecular field analysis (MFA) technique to derive predictive models that may be used to design of multikinase inhibitors.

Method. MFA is one of the 3D–QSAR methods that relate the biological activity of molecules with steric and electrostatic interactions between the compound and the probe atom on a rectangular grid according to Lennard–Jones and Coulomb potentials. MFA studies were performed with the QSAR module of Cerius^2 using genetic partial least squares (G/PLS) algorithm.

Results. MFA was carried out for both KDR and Tie–2 inhibitors and validated using the leave–one–out cross–validation method. These studies produced reasonably good predictive models with high cross–validated (0.831 for KDR, 0.957 for Tie–2) and conventional r^2 (0.979 for KDR, 0.978 for Tie–2) values for both the cases.

Conclusions. The QSAR models developed for KDR and Tie–2 inhibitors show good correlation and predictive ability based on which biological activities for the new molecules can be predicted. Molecules with dual inhibitory activity against both KDR and Tie–2 would show synergistic effects by affecting critical stages of blood vessel formation, and thus potentially leading to a new approach to cancer therapy.

Keywords. Receptor tyrosine kinases; 3–D QSAR; MFA; molecular field analysis; cancer.

Abbreviations and notations

GFA, genetic function approximation	PRESS, predicted sum of squares
G/PLS, genetic partial least squares	RTK, receptor tyrosine kinases
KDR, kinase insert domain containing receptor	Tie–2, tyrosine kinase with immunoglobulin and epidermal growth factor homology domains–2
LOO, leave one out	VEGFs, vascular endothelial growth factors
MFA, molecular field analysis	3D–QSAR, three–dimensional quantitative structure–property relationships
MCSG, maximum common subgroup	
PLS, partial least squares	

* Correspondence author; E–mail: omsilakari@rediffmail.com.

1 INTRODUCTION

Receptor tyrosine kinases (RTK) represent a large family of membrane bound enzymes responsible for a diverse range of biological processes, including relay of angiogenic signals from tumor secreted growth factors [1]. Angiogenesis, the formation of new blood vessels from existing vasculature [2] has been considered a critical event for the growth and metastasis of solid tumors because blood is essential for solid tumors to manage nutritional supplies and waste removal. KDR and Tie–2 are of particular interest since their receptors are expressed primarily on endothelial cells and play a direct role in such angiogenic processes.

KDR and its ligands vascular endothelial growth factors (VEGFs) play crucial roles in vessel sprouting and new vessel initiation in early stages of angiogenesis through induction of proliferation, migration and survival of endothelial cells [3–5]. Similar to KDR, Tie–2 and its ligands angiopoietins play an important role in stabilizing the immature endothelial cell network, attracting pericytes, maintaining biochemical interactions and vessel integrity, which are thought to be implemented in secondary stages of blood vessel formation [6–8].

As angiogenesis is a major event in cancer growth and proliferation, RTK inhibitors as a target for anti–angiogenesis can be aptly applied as a new mode of cancer therapy. To explore the substitutional requirements for dihydroindazolocarbazole analogues as RTK inhibitors and to obtain highly predictive models, 3D–QSAR analysis was performed using the most widely used computational tool, molecular field analysis (MFA) by considering the steric and electrostatic influences [9]. The derived models will give insight to the influence of various interactive fields on the activity and thus aid in designing multikinase inhibitors having dual KDR and Tie–2 inhibitory activity in the hope that these molecules may be further explored as anticancer agents.

2 MATERIALS AND METHODS

2.1 Biological Data and Structures

The activity data and two–dimensional structures of C–3 N–urea, amide, and carbamate dihydroindazolo[5,4–α]pyrrolo[3,4–*c*]carbazole analogues reported as RTK inhibitors was collected from literature [10]. The activity data and structure of each molecule are listed in Table 1. Biological activities were converted into the corresponding pIC_{50} values (–log IC_{50}), where IC_{50} value represent the drug in molar concentration that causes 50% inhibition of enzyme. These molecules were divided into two sets, namely training set for generation of models and test set for determination of validity of models. Training set includes 26 molecules for both KDR and Tie–2 and test set have 5 molecules for KDR and 6 for Tie–2.

2.2 Molecular Structure Generation and Alignments

Molecular modeling analysis was performed using Cerius^2 software [11]. The structures of the compounds were built using molecular sketcher facilities provided in the modeling environment of Cerius^2. Geometric optimization was carried using DREIDING force field [12]. Partial atomic charges were calculated using the charge equilibration method [13]. Multiple conformation of each molecule was generated using the Boltzmann jump as a conformational search method. All molecules were initially energy minimized with smart minimizer and further geometric optimization of each molecule was carried out with MOPAC 6 package using the semi–empirical AM1 (Austin Model) Hamiltonian [14].

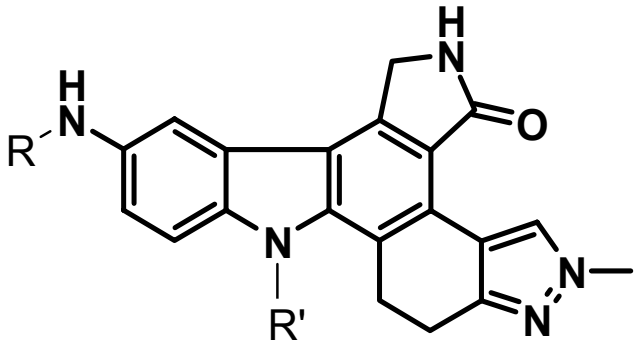

Figure 1. Basic scaffold dihydroindazolocarbazole shown in bold which is used as the template for the superimposition of the rest of the molecules.

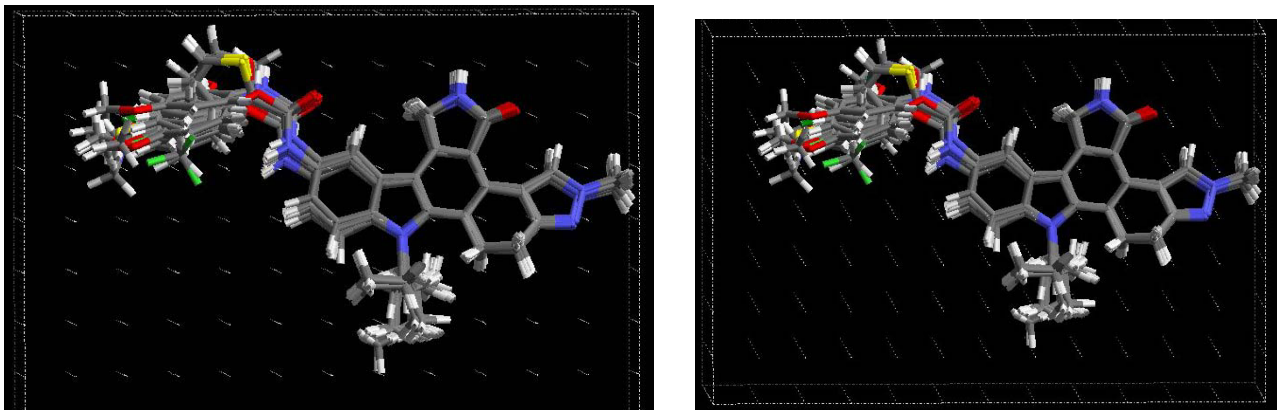

(*a*) (*b*)

Figure 2. The stereoview of aligned molecules of the training set for KDR (a) and Tie–2 (b) inhibitors.

All the molecules were aligned to bold faced portion of the most active molecule, compound **31** for KDR and compound **12** for Tie–2 by considering the significant basic scaffold dihydroindazolocarbazole shown in Figure 1. The method used for performing the alignment was maximum common subgroup (MCSG) [11]. This method looks at molecules as points and lines, and uses the techniques of graph theory to identify patterns. It finds the largest subset of atoms in the shape reference compound that is shared by all the structures in the study table and uses this subset for alignment. The stereoview of aligned molecules is shown in Figure 2.

Table 1. Molecular structure and inhibitory activity data for KDR and Tie–2 RTK inhibitors

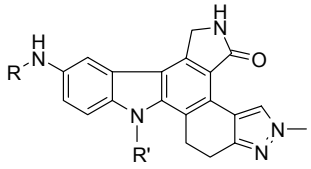

No	R	R'	KDR IC_{50} (nM)[a]	KDR pIC_{50}[b]		Tie–2 IC_{50} (nM)[a]	Tie–2 pIC_{50}[b]	
				Obs	Pred		Obs	Pred
1[d]	H		9	8.046	8.112	36	7.444	7.426
2	H		11	7.959	7.957	48	7.319	7.395
3	H	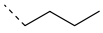	88	7.056	7.028	230	6.638	6.578
4[d]	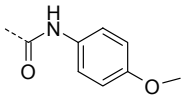					4	8.398	8.078
5[c]	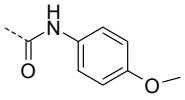		16	7.796	7.889	2	8.699	8.695
6	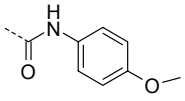		18	7.745	7.790	3	8.523	8.488
7	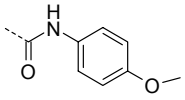	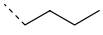	101	6.996	7.015	7	8.155	8.215
8[d]	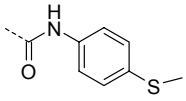		14	7.854	7.801	3	8.523	8.102
9[c,d]	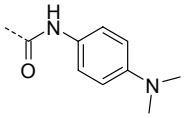		24	7.620	7.131	6	8.222	8.122
10	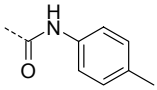		8	8.097	8.133	3	8.523	8.534
11	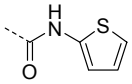		21	7.678	7.812	19	7.721	7.773
12	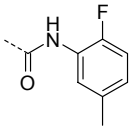		29	7.538	7.539	1	9.000	8.927
13	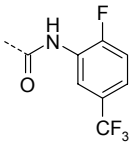		159	6.799	6.818	4	8.398	8.470
14	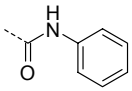		16	7.796	7.835	5	8.301	8.438
15	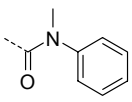		7	8.155	8.030	2	8.699	8.579

Table 1. (Continued)

No	R	R'	KDR IC_{50} (nM)[a]	KDR pIC_{50}[b]		Tie–2 IC_{50} (nM)[a]	Tie–2 pIC_{50}[b]	
				Obs	Pred		Obs	Pred
16	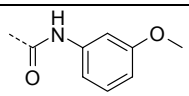		25	7.602	7.562	4	8.398	8.524
17	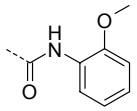		41	7.387	7.512	8	8.097	8.164
18	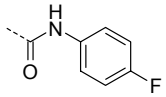		12	7.921	7.870	2	8.699	8.686
19	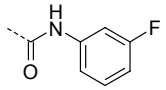		12	7.921	7.844	2	8.699	8.537
20[c,d]	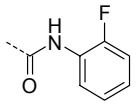		9	8.046	8.053	2	8.699	8.395
21	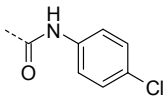		48	7.319	7.228	6	8.222	8.273
22	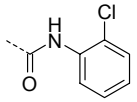		9	8.046	8.077	3	8.523	8.479
23	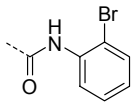		10	8.000	8.043	4	8.398	8.443
24	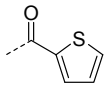		4	8.398	8.479	12	7.921	7.933
25	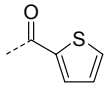		7	8.155	8.111	10	8.000	8.017
26	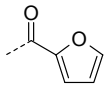		3	8.523	8.552	29	7.538	7.535
27	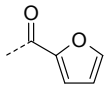		5	8.301	8.255	20	7.699	7.659
28	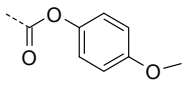		12	7.921	7.906	5	8.301	8.306
29[c d]	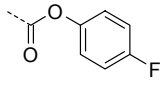		46	7.337	7.684	11	7.959	8.195
30[c]	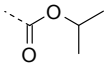		5	8.301	8.414	11	7.959	7.967
31	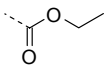		2	8.699	8.562	18	7.745	7.720
32	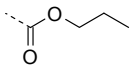		3	8.523	8.566	7	8.155	7.994

[a] IC_{50} values collected from literature; [b] $pIC_{50} = -\log IC_{50} = \log 1/ IC_{50}$
[c] KDR inhibitor test set; [d] Tie–2 inhibitor test set

2.3 Molecular Field Analysis

Molecular field values were generated for all the aligned molecules using CH_3 (steric) and H+ (electrostatic) probes. Only 10% from the total number of variables, whose variance is highest, were considered as independent variables. The biological activities of all 26 molecules in training set for both KDR and Tie–2 were used as dependent variables. The regression analysis of data was performed using G/PLS techniques available in QSAR+ environment of Cerius^2 software. G/PLS is derived from two QSAR calculation methods: genetic function approximation (GFA) and partial least squares (PLS). Both GFA and PLS have been shown to be valuable tools in cases where the data set has more descriptors than samples. The G/PLS algorithm uses GFA to select appropriate basis functions to be used in a model of the data and PLS regression as the fitting technique to weigh the basis functions relative contributions in the final model [15]. For deriving the MFA QSAR equations, number of compounds in training set are 26, the descriptor values scaled to a variance of 1.0, the optimal number of components fixed as 5, the length of the equation set to 9 terms and genetic crossovers limited to 50000 generations. Cross–validation was performed with the leave–one–out procedure.

3 RESULTS AND DISCUSSION

The MFA models were built and validated based on internal prediction of training set and external prediction of the test set. G/PLS was carried out over 50000 generations with a population size of 100. The statistical results of the best MFA models are given in equation 1 for KDR and equation 2 for Tie–2 inhibitors. In these equations the steric (CH_3) and electrostatic (H^+) descriptors, specify the regions where variations in the structural features (steric or electrostatic) of different compounds in the training set, lead to increased or decreased inhibitory activities. The number accompanying descriptors represents its position in the three–dimensional MFA grid. An energy cutoff of –30 to +30 kcal/mol was set for both steric and electrostatic contributions. The smoothing parameter d was set to 1.0 to control the bias in the scoring factors between equations with different number of terms.

$$\begin{aligned}\text{Activity (KDR inhibitors)} = {} & 7.77044 - 0.034846(CH_3/222) \\ & - 0.035361(CH_3/389) + 0.016837(H^+/165) + 0.007651(H^+/367) - 0.026451(CH_3/230) \\ & - 0.015383(H^+/719) + 0.016135(CH_3/236) - 0.016947(CH_3/111)\end{aligned} \quad (1)$$

$$\begin{aligned}\text{Activity (Tie–2 inhibitors)} = {} & 6.9508 + 0.007995(CH_3/167) \\ & + 0.019362(CH_3/241) + 0.016334(CH_3/731) - 0.007327(H^+/465) + 0.010901(H^+/398) \\ & - 0.016682(CH_3/445) + 0.012405(CH_3/231) + 0.010775(H^+/166)\end{aligned} \quad (2)$$

The significance of G/PLS models was judged by various statistical parameters, namely the number of molecules *n* greater than 20, squared correlation coefficient of determination r^2 greater than 0.7 describes significance of a model. The index r^2 is a relative measure of quality of fit of the model. Its value depends on the overall variance of the data. The generated QSAR equations were

internally validated by leave–one–out (LOO) cross–validation. A cross validation coefficient q^2 of greater than 0.5 shows good internal predictivity of the model. A boot strapped correlation coefficient r^2_{bs} is an independent measure of stability of model. A calculated r^2_{bs} closer to conventional r^2 indicates the stability of generated models. Further more, the external predictive power of the model was validated with test set compounds i.e. predicted correlation coefficient r^2_{pred} which should be greater than 0.5 [16]. The statistical parameters for the two MFA models developed are given in Table 2.

Table 2. Statistical Parameters of MFA Models

Parameter	KDR	Tie–2
Data points (*n*)	26	26
Correlation coefficient (*r*)	0.990	0.989
Square correlation coefficient (r^2)	0.979	0.978
Cross validated correlation coefficient (q^2)	0.831	0.957
Predicted sum of squares (*PRESS*)	0.959	0.282
Optimum number of components (*N*)	5	5
Predicted correlation coefficient (r^2_{pred})	0.580	0.728
Bootstrapped correlation coefficient (r^2_{bs})	0.949	0.973
Least square error (*LSE*)	0.004	0.005

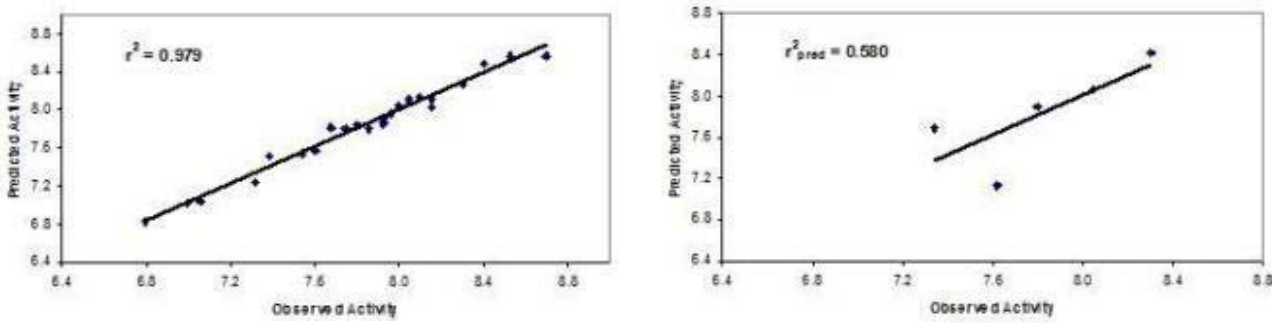

(*a*) (*b*)

Figure 3. Correlation graph for training set (*a*) and test set (*b*) for the best MFA model for KDR inhibitors.

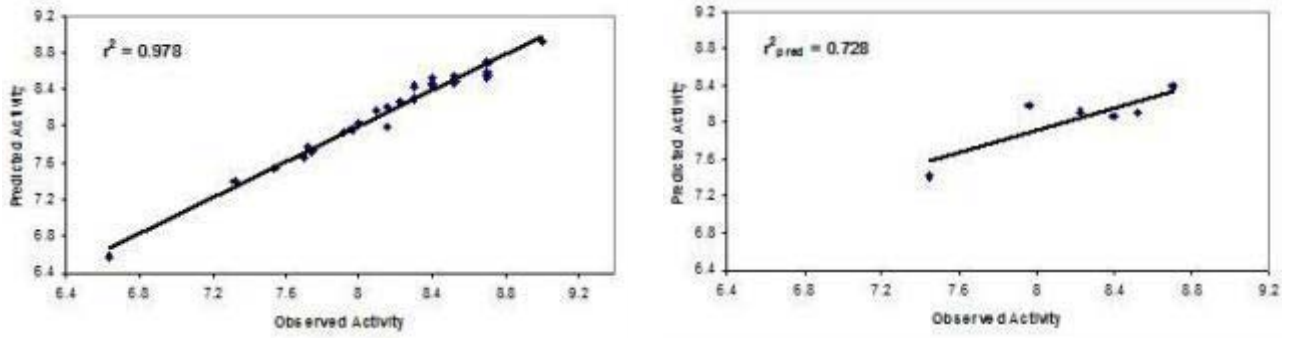

(*a*) (*b*)

Figure 4. Correlation graph for training set (*a*) and test set (*b*) for the best MFA model for Tie–2 inhibitors.

G/PLS analyses of the KDR inhibitors showed r^2 = 0.979, r^2_{bs} = 0.949, and cross validated q^2 = 0.831. The prediction of the model was reasonably good with an r^2_{pred} = 0.580. G/PLS analyses of Tie–2 inhibitors showed r^2 = 0.989, r^2_{bs} 0.973, q^2 = 0.957, and r^2_{pred} = 0.728. Figures 3 and 4 show the correlation graphs between observed and predicted activities from the best MFA models for training set and test set molecules for KDR and Tie–2 inhibitors.

(*a*) (*b*)

Figure 5. The stereoview of MFA model and the interaction points. (*a*) The most active compound **31** (KDR inhibitor) is displayed in background as reference. (*b*) The most active compound **12** (Tie–2 inhibitor) is displayed in background as reference.

The best MFA models derived from the G/PLS technique are presented in Figure 5. The most potent inhibitors of respective enzymes are displayed in the background: compound **31** for KDR in map (*a*); compound **12** for Tie–2 in map (*b*) to demonstrate its affinity for the steric and electrostatic regions of inhibitors. The steric descriptor with a positive or negative coefficient shows a region where bulky substituent is favored or disfavored respectively. The electrostatic descriptor with a positive coefficient indicates, region favorable for electropositive group while a negative coefficient indicates that an electronegative or electron withdrawing group is required at the position. In Figure 5(a) presence of steric descriptor CH_3/389 with negative coefficient shows less bulky group is favorable for KDR activity at this position. This explains the low activity of compound **3** and **7** having *n*–butyl chain at R'. Compound **4** having ethyl at R' position was not predicted well and deleted from the test set. Thus, from these data the optimal alkyl group for the N–13 nitrogen (R') appeared to be *n*–propyl or *i*–butyl. Appearance of steric descriptors CH_3/111, CH_3/222, CH_3/230 with negative coefficient indicates presence of sterically unfavorable zone. As in compounds **12** and **13** having substituted phenyl urea at R shows lesser KDR inhibitory activity. Electropositive descriptor H+/367 with positive coefficient shows electropositive group are favorable at this position. Presence of steric descriptor CH_3/236 with positive coefficient explains good inhibitory activity of carbamate derivatives **30**, **31**, **32** having alkyl chain.

In Figure 5(*b*) presence of steric descriptor CH_3/445 with negative coefficient indicates presence of sterically unfavourable region as evident by low Tie–2 inhibitory activity of compound **3**. This shows that optimal alkyl group at R' is *n*–propyl or *i*–butyl as required for KDR inhibitors. Appearance of electronic descriptor H+/465 with negative coefficient and H+/398 with positive coefficient indicates subtle balance of electronegative nitrogen atom and electropositive hydrophobic alkyl chain. Appearance of steric descriptors CH_3/241, CH_3/167, CH_3/231 with positive coefficient indicates presence of sterically bulky group is favorable. This is explained by substituted phenyl urea and amide derivatives (**4**–**10**, **12**, **13**, **16**–**23**, **28**) which show good Tie–2 inhibitory activity.

4 CONCLUSIONS

The development of RTK inhibitors is an active area of drug discovery research within the pharmaceutical industry. The 3D–QSAR studies carried out using MFA was applied to rationalize the KDR and Tie–2 activity to various dihydroindazolocarbazole analogues. This study yielded stable and statistically significant models with high correlation coefficients. An analysis of MFA models for KDR and Tie–2 RTK have led to identification of some of the important regions of the inhibitor that possess specific steric and electrostatic interactions with two different kinases.

Overall, the present 3D–QSAR study investigates the indispensable structural features of various dihydroindazolocarbazole analogues and will provide valuable tools for guiding the rational design of novel inhibitors and for predicting their biological activity for the two RTK subtypes prior to chemical synthesis and biological evaluation. The generated new molecules are expected to have dual inhibitory activity for KDR and Tie–2 RTK for prevention of variety of cancer.

5 REFERENCES

[1] L. K. Shawver, K. E. Lipson, T. A. T. Fong, G. McMahon, G. D. Plowman, and L. M. Strawn,. Receptor tyrosine kinases as targets for inhibition of angiogenesis, *Drug Discovery Today* **1997**, *2*, 50–63.
[2] W. Risau, Mechanism of angiogenesis, *Nature* **1997**, *386*, 671–674.
[3] F. Shalaby, J. Rossant, T. P. Yamaguchi, M. Gertsenstein, X. F. Wu, M. L. Breitman, and A. C. Schuh, Failure of blood–island formation and vasculogenesis in Flk–1–deficient mice, *Nature* **1995**, *376*, 62–66.
[4] P. Carmeliet, V. Ferreira, G. Breier, S. Pollefeyt, L. Kieckens, M. Gertsenstein, M. Fahrig, A. Vandenhoeck, K. Harpal, C. Eberhardt, C. Declercq, J. Pawling, L. Moons, D. Collen, W. Risau, and A. Nagy, Abnormal blood vessel development and lethality in embryos lacking a single VEGF allele, *Nature* **1996**, *380*, 435–439.
[5] N. Ferrara, and T. Davis–Smyth, The biology of vascular endothelial growth factor, *T. Endocr. Rev.* **1997**, *18*, 4–25.
[6] I. Kim, H. G. Kim, S. O. Moon, S. W. Chae, J. N. So, K. N. Koh, B. C. Ahn, and G. Y. Koh, Angiopoietin–1 Induces Endothelial Cell Sprouting through the Activation of Focal Adhesion Kinase and Plasmin Secretion, *Circ. Res.* **2000**, *86*, 952–959.
[7] S. Davis, T. H. Aldrich, P. F. Jones, A. Acheson, D. L. Compton, V. Jain, T. E. Ryan, J. Bruno, C. Radziejewski, P. C. Maisonpierre, S. Davis, T. N. Sato, and G. D. Yancopoulos, Isolation of angiopoietin–1, a ligand for the tie2 receptor by secretion–trap expression cloning, *Cell* **1996**, *87*, 1161–1169.
[8] C. Suri, P. F. Jones, S. Patan, S. Bartunkova, P.C. Maisonpierre, S. Davis, T. N. Sato, and G. D. Yancopoulos,

Requisite role of angiopoietin–1, a ligand for the tie2 receptor, during embryonic angiogenesis, *Cell* **1996**, *87*, 1171–1180.
[9] A. J. Hopfinger and J. S. Tokarsi, *Practical Applications of Computer–Aided Drug Design*; in: P. S. Charifson, Eds. Marcel Dekker: New York, **1997**, pp 105–164.
[10] N. C. Becknell, A. L. Zulli, T. S. Angeles, S. Yang, M. S. Albom, L. D. Aimone, C. Robinson, H. Chang, and R. L Hudkins, Novel C–3 N–urea, amide, and carbamate dihydroindazolo [5,4–α] pyrrolo [3,4–c] carbazole analogues as potent tie–2 and VEGFR–2 dual inhibitors, *Biorg. & Med. Chem. Lett.* **2006**, *16*, 5368–5372.
[11] Cerius^2 Molecular Modeling Program Package, Molecular Simulations (Accelrys) Inc.: San Diego, CA 92121–3752. USA.
[12] S. L. Mayo, B. D. Olafson, and I. Goddard, DREIDING: a generic force field for molecular simulations. *J. phys. Chem.* **1990**, *94*, 8897–8909.
[13] A. K. Rappe, and W. A. Goddard III, Charge equilibration for molecular dynamics simulations, *J. Phys. Chem.* **1991**, *95*, 3358–3363.
[14] M. J. S. Dewar, E. G. Zoebisch, E. F. Healy, and J. J. P. Stewart, AM1: A New General Purpose Quantum Mechanical Molecular Model, *J. Am. Chem. Soc.* **1985**, *107*, 3902–3909.
[15] S. Wold, In: *Chemometric Methods in Molecular Design*, Eds. van de Waterbeemd H, VCH, Weinheim, 1995, Vol. 2, pp 195–218.
[16] Quantitative Structure Activity Relationship (QSAR), VLife Sciences Technologies Pvt. Ltd., www.vlifesciences.com.

Biographies

Neha Kansal has completed B. Pharm. at Guru Jambheshwar University, Hisar, Haryana, India. Then she moved to the Department of Pharmaceutical Science and Drug Research, Punjabi University, Patiala, Punjab, India, and pursuing the M. Pharmacy degree. Her research interests include rational drug design, CADD, 3D– QSAR, docking, pharmacophore mapping, and synthetic work.

Om Silakari is lecturer in the Division of Pharmaceutical Chemistry at Department of Pharmaceutical Science and Drug Research, Punjabi University, Patiala, Punjab, India. After obtaining a Ph.D. degree in Pharmacy from Dr. H S Gour University, Sagar, India. Dr. Silakari supervising many PG students in the field of QSAR, rational drug design, and synthetic chemistry and published research papers in the field of QSAR.

Muttineni Ravikumar is a scientist in GVK Biosciences, Hyderabad, India. He did his M. Tech from Department of Chemical Engineering, Andhra University, Vishakhapatnam, A.P. India. . His research interests include rational drug design, CADD, 3–D QSAR, docking, pharmacophore mapping, and synthetic work, and published research papers in the various reputed journal.